Variable wavelength interferometry
II. Uniform-field method for transmitted light *

MAKSYMILAN PLUTA

Central Optical Laboratory, ul. Kamionkowska 18, 03–805 Warszawa, Poland.

A new interferometric method — the variable wavelength interferometry (VAWI) has been developed. In a previous paper the fringe-field version of this method was presented. Now, the uniform-field VAWI technique is discussed. The latter seems to be sometimes more useful and accurate than the fringe-field technique, especially when cylindrical, round, spherical or lens-like objects are to be examined.

1. Introduction

In the previous paper [1] the variable wavelength interferometry (VAWI) with fringe-field for transmitted light has been presented. Now, the uniform-field version of the VAWI is discussed. This version is sometimes more useful and accurate than the fringe-field method, especially when small round objects are to be examined.

In general, uniform-field interference can be considered as fringe-field interference when interference fringes are infinitely extended in the empty field of view of the interferometer. The theory of the VAWI given previously for the fringe-field method is therefore valid for the uniform-field method as well, and this article should be read together with paper [1].

2. Theoretical background

Let a transparent object, e.g. a disc-like plate, be placed in the object plane of a light-transmitting two-beam interferometer adjusted to uniform-field interference in the image plane. We assume that the object and its surrounding medium are characterized by typical curves of the spectral dispersion of the refractive index (see Fig. 1 in [1]). The optical path difference δ produced by the object is given by the relation $\delta = (n' - n) t$, where n and t are the refractive index and the thickness of the object, respectively, and n' is the refractive index of the surrounding medium.

Without restricting in any way the generality of the results, we can assume that for the zero interference order ($m = 0$) the background B (Fig. 1) of the field of
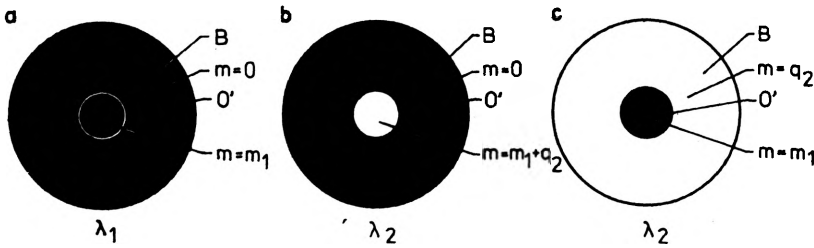

Fig. 1. Principle of the uniform-field VAWI method

view of the interferometer is dark; this is, for instance, the case of the polarization interference system whose polarizer and analyser are crossed.

In under above assumptions the optical path difference δ is greater than the light wavelength λ, then interference patterns occur as shown in Fig. 1. For a particular wavelength λ_1 the darkness of the interference image O' of the object is the same as that of the background B of the zero interference order (Fig. 1a). When the wavelength of monochromatic light becomes shorter or longer than λ_1, the image O' changes its intensity and a missmatching in brightness arises between the background B and the object image (Fig. 1b). This situation may be described, in general, by the same equations as previously for the fringe interference method [1]:

$$\delta_1 = (n'_1 - n_1)t = m_1 \lambda_1, \tag{1a}$$

$$\delta_2 = (n'_2 - n_2)t = (m_1 + q_2)\lambda_2 \tag{1b}$$

where the indices 1 and 2 refer to two different wavelengths λ_1 and λ_2, q_2 is a fraction number or an integer, and m_1 is an unknown integer which expresses the interference order within the object image O'. The whole number m_1 is referred to as the introductory or initial interference order. Consequently, the quantity $m_1 + q_2$ expresses the current interference order within the object image O'. The parameter q_2 may be positive or negative. In the first instance ($q_2 > 0$) the wavelenth λ_2 is shorter than λ_1, while in the second ($q_2 < 0$) – the wavelength λ_2 is longer than λ_1. The positive q_2 expresses an increment while $q_2 < 0$ expresses a decrement of the interference order with respect to m_1.

The optical path differences δ_1 and δ_2 may also be expressed by the following relations:

$$\delta_1 = (n'_1 - n)t = \frac{C_1}{b_1}\lambda_1, \tag{2a}$$

$$\delta_2 = (n'_2 - n_2)t = \frac{C_2}{b_2}\lambda_2 \tag{2b}$$

where b_1 and b_2 are the constant parameters for a given interference system adjusted to the uniform-field interferometry, whereas C_1 and C_2 are directly connected with the optical path differences δ_1 and δ_2. All these parameters can be

measured by means of a phase compensator. If Δ denotes the optical path difference introduced by the phase compensator, then the relationship between the intensity I of the interference field and Δ is a squared sine function, such as that shown in Fig. 2. The parameter b is simply, for a given wavelength λ, the distance between two successive minima (or maxima) of the light intensity. The shorter wavelength λ the smaller b, but λ/b is a constant (if the optical system of the interferometer does not suffer from the material optical dispersion). On the other hand, the parameter C is given by such a positive or negative value of Δ which is necessary to cancel completely the phase difference between interfering waves within the object image O' (Fig. 1). The two parameters, b and C, should be expressed of course in the same units, e.g. in µm.
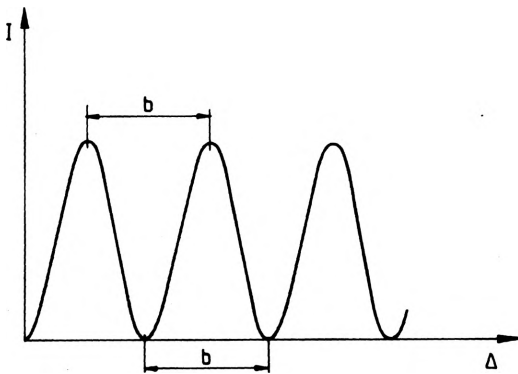

Fig. 2. Light intensity (I) as a function of the optical path difference (Δ) due to the action of a phase compensator

Ruturning to the fringe interference method [1] shows that the parameter b is equivalent to the interfringe spacing, whereas C corresponds with the total deflection (displacement) of interference fringes in the object image.

The measuremt of the paramater C is a common procedure in the conventional uniform-field interferometry. This measurement is possible only when the zero interference order in the image of the object under study can be identified. However, the identification of interference orders is now more trublesome than in fringe interferometry. Fortunately, this does not apply to the VAWI. From Eqs. (1) and (2) it follows that $C_1/b_1 = m_1$ and $C_2/b_2 = m_1 + q_2$; consequently, the measuremt of the parameter C may be replaced by determining m_1 and q_2. Equations (1) yield

$$m_1 = q_2 \frac{\lambda_2}{N_{21} \lambda_1 - \lambda_2} \tag{3}$$

where

$$N_{21} = \frac{n'_2 - n_2}{n'_1 - n_1} = \frac{\delta_2}{\delta_1}. \tag{4}$$

These formulae are indentical with those for the fringe interference method [1].

The parameter q_2 can be expressed as

$$q_2 = \frac{c_2}{b_2} \qquad (5)$$

where c_2 is given by such a value of $\Delta = \Delta_2$ which is necessary to restore the interference order m_1 in the image of the object under study. In other words, introducing Δ_2 makes that the interference image shown in Fig. 1b is transformed into the image shown in Fig. 1c.

If the optical path difference δ is several times greater than λ, the parameter q_2 may be as great as 1, 2, 3, and even more. In this case Eq.(1b) can be developed into several further equations such as follows:

$$\delta_1 = m_1 \lambda_1, \qquad (6a)$$

$$\delta_2 = (m_1 + 1)\lambda_2, \qquad (6b)$$

$$\delta_3 = (m_1 + 2)\lambda_3, \qquad (6c)$$

$$. \quad . \quad . \quad . \quad . \quad . \quad . \quad . \quad . \quad .$$

$$. \quad . \quad . \quad . \quad . \quad . \quad . \quad . \quad . \quad .$$

for $\lambda_1 > \lambda_2 > \lambda_3 \ldots$ if λ_1 is selected in the long-wave region of the visible spectrum.

The situation described by Eqs.(6) is easily recognizable because the image O' (Fig. 1a) is as dark as the background B for the wavelengths $\lambda_1, \lambda_2, \lambda_3, \ldots$ which satisfy Eqs. (6); consequently, the determination of the optical path differences $\delta_1, \delta_2, \delta_3, \ldots$ is reduced to the measurement of these wavelengths alone. This measurement is easily performed using a polarization interference system such as that applied in the wavefront shearing interference microscope Biolar PI [2], which is used here for illustrating the performance of the VAWI methods.

3. Practical implementation

The above-mentioned interference microscope gives both the fringe and uniform interferences in the image plane of the objective. These two possibilities are realized by using different birefringent beam-splitters. The splitter used for the fringe-field interference method is a double-refracting Wollaston prism, while that for the uniform-field interference method is the Nomarski prism (W, Fig. 3). Interference fringes I of the latter are localized in the back focal plane F' of the objective Ob. Requirements for spatially coherent illumination is obtained by using a slit diaphragm localized in the front focal plane of the condenser C. The image S' of the slit S of the condenser diaphragm D is coincident with and parallel to the interference fringes I. In order to obtain an effective uniform-field interference in the image plane Π' of the objective Ob the width w of the slit S should satisfy the following condition [2]:

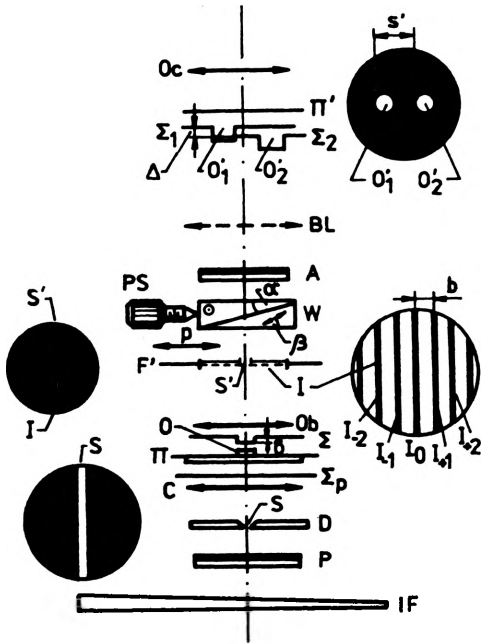$$w < \frac{\lambda}{4} \frac{f_c \mathbf{M}}{s'} \qquad (7)$$

Fig. 3. Schematic diagram of a double-refracting interference system (the Biolar PI) used for the verification of the uniform-field VAWI method. IF — wedge interference system, P — polarizer, D — slit condenser diaphragm, C — condenser, Σ_p — incident plane wavefront, Π — object plane of the objective Ob, O — object under study, Σ — wavefront transmitted by the object, W — Wollaston prism (a version modified by Nomarski), PS — micrometer screw, A — analyser, BL — Bertrand lens used only for observation of interference fringes (I) in the focal plane F' of the objective Ob, Σ_1 and Σ_2 — interfering wavefronts lateraly sheared by the birefringent prism W. Π' — image plane, O'_1 and O'_2 — interference images of the object O, Oc — ocular (for further explanation see the text)

where λ is the wavelength of light used, f_c — the focal length of the condenser C, M — the magnifying power of the objective Ob, and s' — the lateral wavefront shear in the image plane Π'. Moreover, the polarizer P and analyser A must be crossed and their directions of light vibration (PP and AA) should be orientated at an angle of 45° to the slit S.

The birefringent prism W is laterally moved by means of a micrometer drive screw PS. This movement (marked by the arrow p in Fig. 3) introduces a continuously variable optical path difference Δ (or phase shift) between sheared wavefronts Σ_1 and Σ_2. The screw PS is therefore referred to as the phase screw. The relationship between Δ and the lateral position p is linear (Fig. 4). This fact allows the optical path difference δ to be measured by using the lateral displacement of the prism W: consequently, this prism acts as both the beam-splitter and the phase compensator*. When the interference fringe of zero order (I_0) is exactly coincident with the slit image S', the prism W is at zero position ($p = p_0$ and $\Delta = 0$). The transverse movement of the prism, starting from p_0, causes the interference fringes of successive orders ($I_{+1}, I_{+2}, I_{+3}, \ldots$ or $I_{-1}, I_{-2}, I_{-3}, \ldots$) to be brought into coincidence with the image S' of the condenser slit S. The

---

* This fact was originally discussed and applied in practice by the author of this article in 1962 [3, 4], and next it has been rediscovered by HARTMAN et al. in 1980 [5] and used for the quantitative determination of surface topography by Nomarski differential interference contrast microscopy in reflected light.
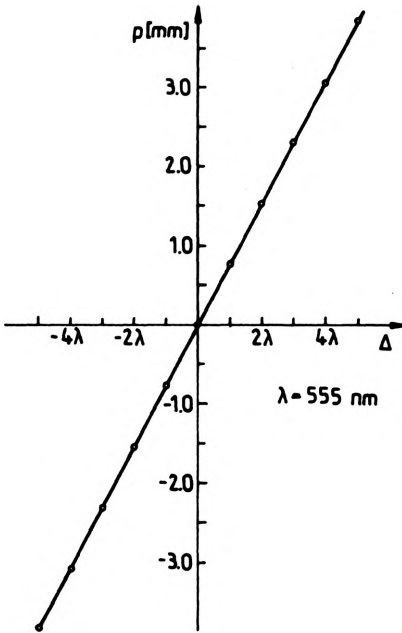
Fig. 4. Optical path difference as a function of the transverse position (p) of the birefringent prism W (see Fig. 3)

interfringe spacing b, and thus the wavelength λ as well, can be measured by means of the micrometer screw PS. The dependence between b and λ is as follows:

$$b = \frac{\lambda}{[(n_e - n_o) + (n'_e - n_o)] \tan \alpha} \tag{8}$$

Here α is the wedge angle of the birefringent prism W, n_o and n_e are the principal (ordinary and extraordinary) refractive indices of the quartz crystal of which the prism W is made, while

$$n'_e = \frac{n_o n_e}{\sqrt{n_o^2 \cos^2 \beta + n_e^2 \sin \beta}}, \tag{9}$$

where β is the angle between the optic axis of quartz and outer surface of lower wedge of the prism W. From the formula (8) it may be seen that the dependence of b upon λ is almost linear (Fig. 5); deviations from the straight line are so small that they are unobservable if highly monochromatic light is used. A detailed discussion of this point may be found in paper [6].

As a matter of fact, the microinterferometer Biolar PI incorporates a combination of two simultaneously acting birefringent prisms. One of them (shown in Fig. 3) is located in a microscope tube, while the other (not shown in Fig. 3) is installed close above the optical system of the objective Ob, and is rotatable round the objective axis. The rotation enables the amount and direction of wavefront shear s' to be changed. The both prisms have the outside localizing planes of their own interference fringes. These fringes are brought into coincidence with the back
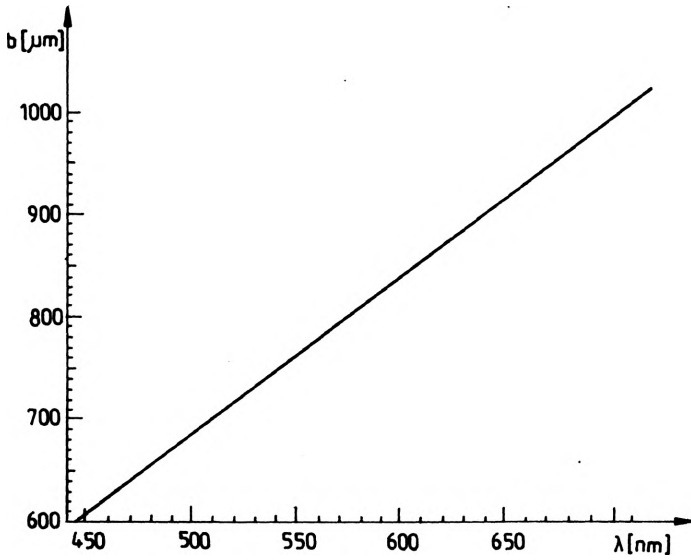
Fig. 5. Relation between the interfringe spacing b and light wavelength λ for the birefringent prism No. 3 of the double refracting interference microscope Biolar PI

focal plane of the objective. The function of the rotatable birefringent prism is not important here and is therefore neglected (for more intensive information, the reader can consult paper [2]).

As a monochromator the wedge interference filter (WIF, Fig. 3) can be used. It is installed before the slit diaphragm D and can be translated in a direction perpendicular to the slit S. No calibration scale of wavelengths is necessary because the peak wavelengths $\lambda_1, \lambda_2, \lambda_3, \ldots$ selected by this filter from a source of white light (halogen lamp 12V/100W) and required for the VAWI method are diectly determined by measuring the interfringe spacings $b_1, b_2, b_3, \ldots$. These wavelengths can be determined with the accuracy $\Delta\lambda = \pm 1$ nm or even better.

4. Expression of the introductory interference order by interfringe spacings

In general, Eqs. (1) can also be given in the form

$$\delta_1 = m_1 k_1 b_1 \tag{10a}$$

$$\delta_2 = (m_1 + q_2) k_2 b_2, \tag{10b}$$

where k_1 and k_2 are the wavelength-dependent coefficients of proportionality,

$$k_1 = \frac{\lambda_1}{b_1}, \tag{11a}$$

$$k_2 = \frac{\lambda_2}{b_2}. \tag{11b}$$

From Eqs. (10) it follows

$$m_1 = q_2 \frac{b_2}{\dfrac{\delta_2}{\delta_1}\dfrac{k_1}{k_2} b_1 - b_2} = q_2 \frac{b_2}{N_{21} k_{12} b_1 - b_2},\tag{12}$$

where $N_{21} = \delta_2/\delta_1$ is defined by Eq. (4), while $k_{12} = k_1/k_2$ expresses the non-linearity between b and λ.

Let Eq. (8) be rewritten as

$$b = \frac{\lambda}{D \tan \alpha},\tag{13}$$

where $D = (n_e - n_0) + (n'_e - n_0)$. This quantity can be referred to as the double refracting power of the birefringent prism (for a typical Wollaston prism $n'_e = n_e$ and $D = 2(n_e - n_0)$. In general, D depends on the wavelength of light due to the spectral dispersion of the birefringence of the quartz crystal of which the double refracting prism is made. Consequently, Eq. (13) may be rewritten, for two different wavelengths λ_1 and λ_2, as follows:

$$b_1 = \frac{\lambda_1}{D_1 \tan \alpha}\tag{14a}$$

$$b_2 = \frac{\lambda_2}{D_2 \tan \alpha}.\tag{14b}$$

By combining Eqs. (11) and (14) we obtain

$$\frac{k_1}{k_2} = k_{12} = \frac{D_1}{D_2}.\tag{15}$$

Table 1 shows the values of k_{12} for different pairs of wavelengths λ_1 and λ_2 with an interval $\Delta\lambda = \lambda_1 - \lambda_2 \geqslant 50$ nm through the visible spectrum. As can be seen, the parameter k_{12} is only slightly smaller than unity, especially in the long-wave region of the spectrum.

In the first part of this work [1] it has been shown that in many situations the coefficient $N'_{21} = 1$, or can be assumed to be equal to unity. In particular, $N'_{21} = 1$ when $n'(\lambda) = $ const and $n(\lambda) = $ const or $n'(\lambda) - n(\lambda) = $ const. In these cases Eqs. (3) and (12) take the form:

$$m_1 = q_2 \frac{\lambda_2}{\lambda_1 - \lambda_2}\tag{16}$$

$$m_1 = q_2 \frac{b_2}{k_{12} b_1 - b_2}.\tag{17}$$

These formulae can also be utilized to many other measuring situations, where the coefficient N_{21} is not exactly but only approximately equal to unity. In these

Table 1. Values of the coefficient k_{12} for different pairs of wavelengths λ_1 and λ_2

λ_1 [nm]	λ_2 [nm]	D_1	D_2	$k_{12} = D_1/D_2$
700	650	0.00899	0.00904	0.99447
700	600	0.00899	0.00910	0.98792
700	550	0.00899	0.00917	0.98037
700	500	0.00899	0.00927	0.96979
700	450	0.00899	0.00940	0.95638
650	600	0.00904	0.00910	0.99340
650	550	0.00904	0.00917	0.98582
650	500	0.00904	0.00927	0.97519
650	450	0.00904	0.00940	0.96170
600	550	0.00910	0.00917	0.99237
600	500	0.00910	0.00927	0.98166
600	450	0.00910	0.00940	0.96808
550	500	0.00917	0.00927	0.98921
550	450	0.00917	0.00940	0.97553
500	450	0.00927	0.00940	0.98617

situations the value m_1 calculated from Eq. (16) or (17) will be slightly greater than it follows from Eq. (3) or (12) if the dispersion curves $n(\lambda)$ and $n'(\lambda)$ tend to diverge in the short-wave region of the visible spectrum. On the other hand, if the curves $n(\lambda)$ and $n'(\lambda)$ tend to converge in the short-wave spectral region, the introductory interference order m_1 calculated from Eq. (16) or (17) is somewhat smaller than it follows from Eqs. (3) and (12). In practice, Eq. (16) or (17) is used rather than (3) or (12), and the selection of the correct order m_1 is additonally confirmed by the analysis of the graphs $\delta(\lambda)$ and coefficients N'_{FC} (or rather N_{FC} relating to air medium) for m_1 increased and diminished by unity. A detailed discussion of this problem has been given in the first part [1] of this work.

5. Experiments

Optical system of the microinterferometer Biolar PI, which has been used here, incorporates three interchangeable birefringent prisms W (Fig. 3) installed in a turret. One of them (No. 2) is for fringe-field interferometry and two other (No. 1 and No.3) for uniform-field interferometry. The prism No. 3 has been selected for the uniform-field VAWI method because this prism varies the optical path difference Δ in a range four times lareger than the prism No. 1.

5.1. Measurement of the core refractive index of an optical fibre

A step-index optical fibre of high numerical aperture was selected as one of the objects especially suitable for the variable wavelength interferometry. Fibres of this kind incorporate cores whose refractive index n is much greater than that (n_{cl}) of
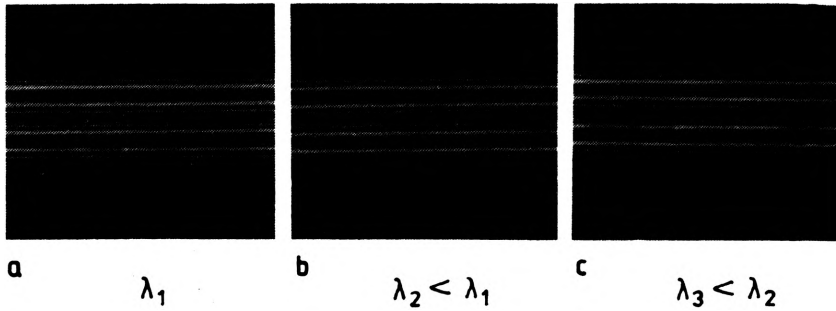
Fig. 6. Uniform-field interference images of an optical fibre; three favourable measuring situations for which interferences orders at the centres of the images are equal to (a) $m = m_1$, (b) $m = m_1 + 1$, and (c) $m = m_1 + 2$.

Table 2. Results of the measurement of the spectral dispersion of the refractive index (n) of the core of a step-index fibre using the uniform-field VAWI method (at 21°C)

	1	2	3
Measuring situation s	1	2	3
Increments q_s	0	1	2
Interfringe spacings b_s [µm]	953,9	774.2	643.5
Wavelengths λ_s [nm]	676.0	558.0	473.0
Refractive indices n'_s	1.5111	1.5177	1.5266
Introductory interference order m_1:			
from Eq. (17)	–	4.7 (=4)	4.7 (=4)
from Eq. (18)	–	4.6 (=4)	4.7 (=4)
Successive interference orders $m_s = m_1 + q_s$	4	5	6
Optical path differences $\delta_s = m_s$ [µm]	2.704	2.790	2.838
Refractive index differences $\Delta n_s = \delta_s/t = \delta_s/17.5$	0.1545	0.1594	0.1622
Refractive indices of the core $n_s = n'_s + \Delta n_s$	1.6656	1.6771	1.6888

$n_C = 1.6672$ $n_D = 1.6737$ $n_F = 1.6866$ $n_F - n_C = 0.0194$ $N_{FC} = (n_F - 1)/(n_C - 1) = 1.0291$

Additional verification of the introductory interference order $m_1 = 4$

Successive interference orders m_s	5 ($m_1 + 1$)	6	7
Optical path differences $\delta_s = m_s \lambda_s$ [µm]	3.380	3.348	3.310
Refractive index differences $\Delta n_s = \delta_s/17.5$	0.1931	0.1913	0.1891
Refractive indices $n_s = n'_s + \Delta n_s$	1.7042	1.7090	1.7157

$n_C = 1.7048$ $n_D = 1.7074$ $n_F = 1.7145$ $n_F - n_C = 0.0097$ $N_{FC} = 1.0138$ impossible

Successive interference orders m_s	3 ($m_1 - 1$)	4	5
Optical path differences $\delta_s = m_s \lambda_s$ [µm]	2.028	2.232	2.365
Refractive index differences $\Delta n_s = \delta_s/17.5$	0.1159	0.1275	0.1351
Refractive indices $n_s = n'_s + \Delta n_s$	1.6270	1.6452	1.6617

$n_C = 1.6300$ $n_D = 1.6402$ $n_F = 1.6590$ $n_F - n_C = 0.0290$ $N_{FC} = 1.0460$ impossible

claddings; they are therefore unsuitable for the conventional interferometry because of the difficulty in the correct identification of interference orders. This does not apply to both the uniform-field and fringe-field VAWI methods.

The optical fibre was placed between a slide and a cover slip, surrounded by a matching liquid, and illuminated at right angles transverse to its axis. The matching liquid was selected so to remove the influence of light refraction at the outer cladding boundary of the fibre, i.e. the condition $n'(\lambda) = n_{cl}(\lambda)$ was fulfilled. Three favourable measuring situations occurred in the red, green and blue regions of the visible spectrum. These situations are shown in Fig. 6 and described by Eqs. 6a, b and c. They manifest themselves by a maximally dark fringe along the centres of the two split interference images of the fibre under study. The result of the measurement of the spectral dispersion of the core refractive index is shown in Table 2 and Figs. 7 and 8.

As can be seen, the initial interference order m_1, which results from Eq. (17) or (18), is found to be equal to 4. This value is also confirmed by an additionl analysis in which m_1 is supposed to be equal to 5 and 3. The curves $n(\lambda)$ for $m_1 = 5$ and $m_1 = 3$ in Fig. 7 are unreal. This also concerns the coefficients $N_{FC}(5)$ and $N_{FC}(3)$; these are so distant from the curve $N_{FC}(n_D)$ shown in Fig. 8 that they cannot represent any optical glasses of which optical fibres are made. Only the curve $n(\lambda)$ for which $m_1 = 4$ and the coefficient $N_{FC}(4)$ are possible.
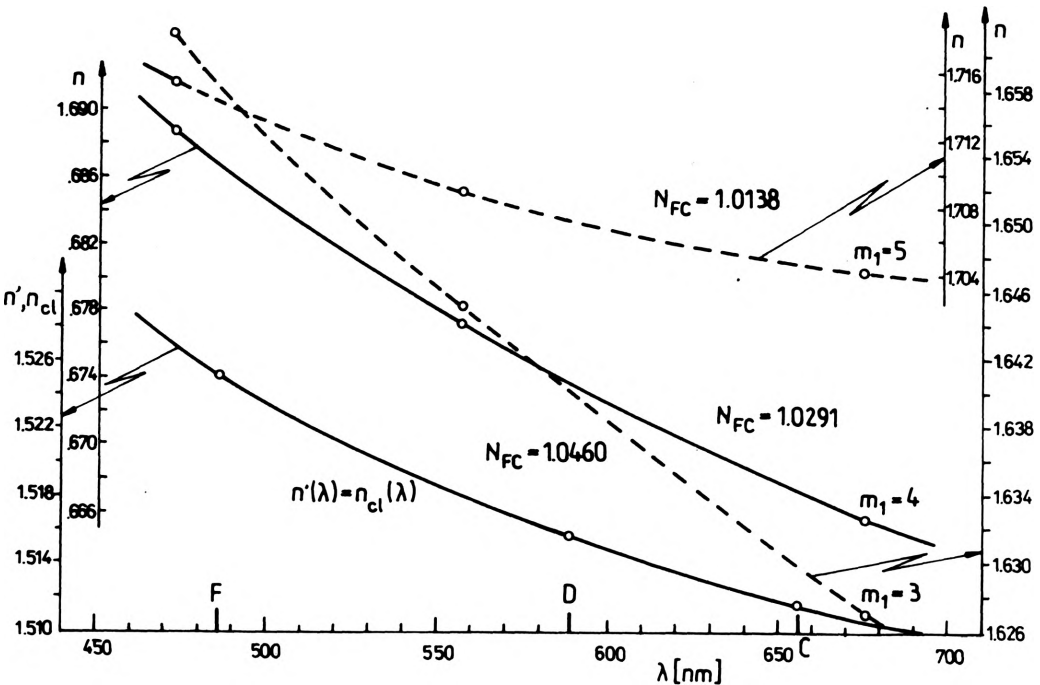

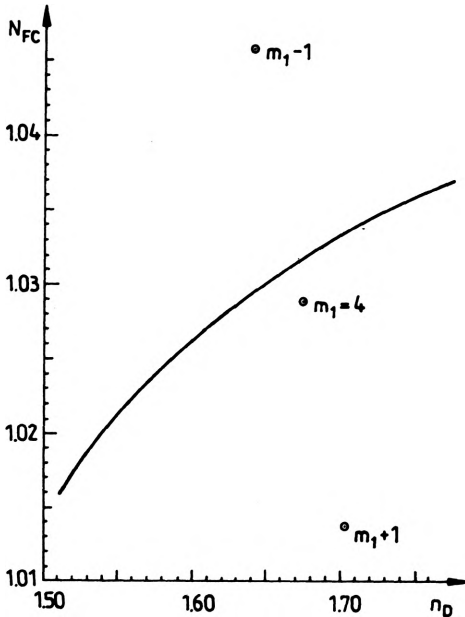Fig. 7. Graphical representation of the results of measurement obtained for a high-aperture optical fibre

Fig. 8. Relation between the dispersion coefficient N_{FC} and refractive index n_D for optical glasses

5.2. Comparison of the uniform-field and fringe-field methods

The same optical fibre was measured using the fringe-field VAWI method described in the first part [1] of this paper. Figure 9 shows the most favourable measuring situations that correspond with the uniform-field interference patterns of Fig. 6. The results are shown in Table 3. As can be seen, the two methods are in agreement with each other; however, the uniform-field interference image of a fibre appears to be more suitable for highly accurate processing using photometric devices. In particular, a photomultiplier photometer with slit aperture enables the increments $q_2 = 0$, 1, 1.5, 2, ... to be fixed extremely precisely.

Table 3. Results of the measurement of the spectral dispersion of the refractive index (n) of the core of a step-index fibre using the fringe-field VAWI method (at 21°C)

| Measuring situations s	1	2	3
Increments q_s	0	1	2
Interfringe spacings b_s [μm]	236.1	190.8	158.7
Wavelengths λ_s [nm]	678.5	557.5	473.0
Refractive indices n'_s	1.5107	1.5177	1.5266
Introductory interference order m_1	–	4.6(=4)	4.6(=4)
Successive interference orders $m_s = m_1 + q_s$	4	5	6
Optical path differences $\delta_s = m_s \lambda_s$ [μm]	2.714	2.788	2.838
Refractive index difference $\Delta n_s = \delta_s/t = \delta_s/17.5$	0.1551	0.1593	0.1622
Refractive index of the core $n_s = n'_s + \Delta n_s$	1.6658	1.6770	1.6888
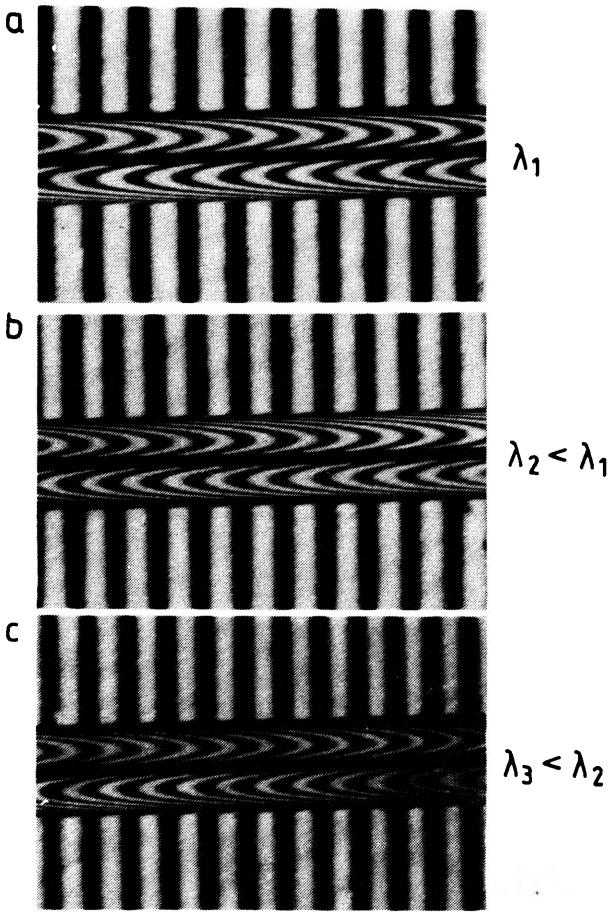
Fig. 9. Fringe-field interference images of the same optical fibre as in Fig. 6

5.3. Measurements of lens-like microobjects

Figure 10a shows a fringe-field interference image of an axially symmetrical lens-like microobject observed through the double refracting interference microscope Biolar PI. Due to the tilt of two laterally sheared wavefronts, the centres of
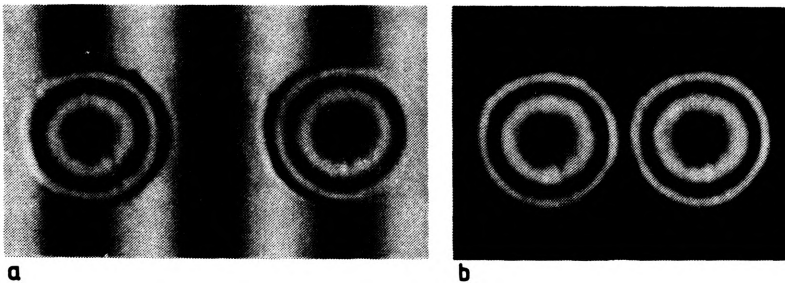

Fig. 10. Fringe-field (a) and uniform-field (b) interference images of a semispherical droplet of Canada balsam

circular fringes within the double image of the object are displaced from the centres of geometrical symmetry. This defect does not occur if the interfering wavefronts are parallel to each other and thus can produce uniform field interference (Fig. 10b). The latter, however, suffers from some difficulty in the identification of interference orders. Fortunately, this difficulty does not apply to the VAWI technique.

A preparation of lens-like microobjects was obtained by heating small particles of powdered Canada balsam deposited on a glass slide. After cooling the balsam droplets can take the form of semi-spherical lenses. One of them (Fig. 11) was selected to determine the spectral dispersion of its refractive index n from the relation $\delta(\lambda) = t[n(\lambda) - n'(\lambda)]$, where $\delta(\lambda)$ is the measured optical path difference, t is the thickness of the droplet at its peak point where δ is measured, and n' is the refractive index of the surrounding medium. In order to obtain $n(\lambda)$ from the above relation, the thickness t should be known or determined simultaneously with δ. Consequently, the double immersion procedure was applied. This gives (for
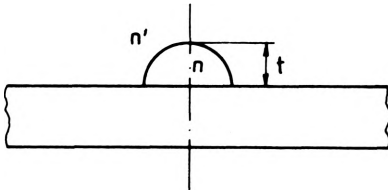

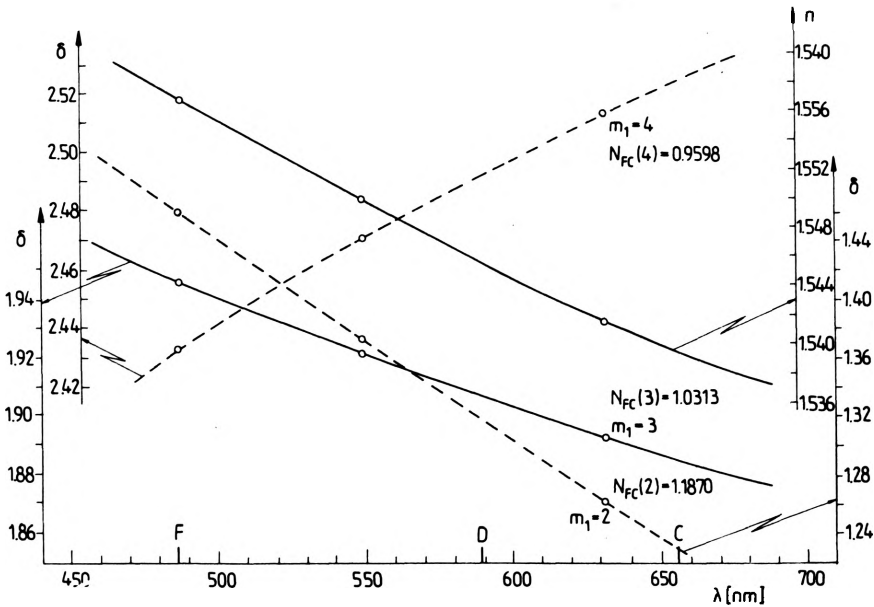Fig. 11. Canada balsam droplet whose interference images are shown in Fig. 10

Fig. 12. Graphical representation of the measuring results obtained for the Canada balsam droplet shown in Fig. 11

Table 4. Results of the measurement of the thickness (t) and spectral dispersion of refractive index of a droplet of Canada balsam using the uniform-field VAWI method (at 22°C)

	Air surrounding medium			Liquid medium
Measuring situation s	1	2	3	1
Increments q_s	0	0.5	1	0
Interfringe spacings b_s [μm]	885.6	759.9	664.2	702
Wavelengths λ_s [nm]	631.0	549.0	486.5	510
Refractive indices of the immersion media	1	1	1	1.5540
Initial interference order m_1	—	3.4(=3)	3.4(=3)	0
Successive interference orders $m_s = m_1 + q_s$	3	3.5	4	0
Optical path differences $\delta_s = m_s \lambda_s$ [μm]	1.893	1.922	1.946	0

Optical path difference δ read out from the graph 1 in Fig. 12 for $\lambda = 510$ nm and air medium $\delta = 1.937$ μm, thickness t of the droplet, calculated from Eq. (18), $t = 1.937/0.554 = 3.496$ μm

| Refractive indices $n = 1 + \delta_s/t$ | 1.5415 | 1.5498 | 1.5566 | |

each wavelength λ) two equations: $\delta' = t(n - n')$ and $\delta'' = t(n - n'')$, from which the thickness t can be calculated

$$t = \frac{\delta' - \delta''}{n'' - n'}. \tag{18}$$

The first immersion medium was air ($n' = 1$), and next the space between the slide and cover slip was filled with Cargille liquid of known refractive index dispersion $n''(\lambda)$. The results obtained are shown in Table 4 and Fig. 12.

6. Conclusions

The uniform-field VAWI method is generally suitable for measuring round or cylindrical objects. In many instances, it appears to be more accurate than the fringe-field method.

The most favourable measuring situations are those for which the interference order increment q is equal 0, 0.5, 1, 1.5, 2, 2.5, ... Such situations occur when the optical path difference to be measured is greater than, say, 1 μm.

A double refracting interference system, such as that on which the microinterferometer Biolar Pl is based, is especially suitable for use of the VAWI methods to a variety of interferometric problems. When the increment $q = 0$, 0.5, 1, 1.5, 2, ... the only measured parameter is the interfringe spacing b which can be determined extremely precisely by measuring its multiple value, say, $10b$. If the polarizer and analyser of the microinterferometr Biolar PI are crossed, then for $q = 0, 1, 2, 3, ...$ the double interference image of the object under study is maximally dark at the points where the optical path difference δ is measured (Fig.

13a). On the other hand, if $q = 0.5, 1.5, 2.5, \ldots$ the points mentioned above become maximally bright (Fig. 13b). The visual estimation of the maximum brightness is less accurate than the maximum darkness. However, rotating the polarizer through an angle of $90°$ reverses the contrast (Fig. 13c) and bright areas of the object image become dark. Consequently, the measuring situations for which $q = 0.5, 1.5, 2.5, \ldots$ may be optimized.
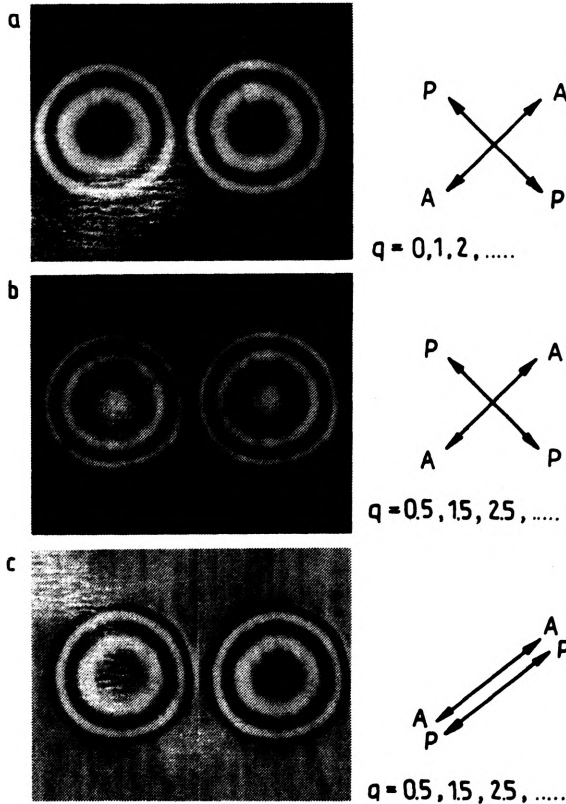

Fig. 13. Uniform-field interference images of the droplet shown in Fig. 11 (for further explanation see the text)

If, however, δ is smaller than or comparable with the light wavelength, the increment q cannot be greater than 0.5, and in this case q is unsuitable for visual estimation and must be measured. In general, such a situation is less convenient than those for which $q = 0.5, 1, 2, 3, \ldots$. Fortunately, there is no problem in the identification of interference orders when δ is small, say, not greater than one light wavelength.

References

[1] Pluta M., Optica Applicata 15 (1985), 375.
[2] Pluta M., Optica Acta 18 (1971), 661.

[3] PLUTA M., Pomiary, Automatyka, Kontrola **8** (1962), 229 and 372 (in Polish).
[4] PLUTA M., J. Sci. Instrum. (J. Phys. E) **2** (1969), 685.
[5] HARTMAN J. S., GORDON R. L., LESSOR D. L., Appl. Opt. **19** (1980), 2998.
[6] PLUTA M., Optica Applicata **12** (1982), 19.

Интерферометрия с плавно переменной длиной волны.
II. Метод однородного поля для проходящего света

Разработан новый интерферометрический метод. В предыдущей статье был представлен полосатый вариант этого метода. В настоящей статье, в свою очередь, представлен вариант однородной интерферометрии с плавно переменной длиной волны. Этот вариант иногда полезнее и точнее, чем вариант с полосатым полем, особенно тогда, когда исследуются цилиндрические, сферические или линзовидные объекты.